

Simulation of propeller hub vortex flow *

Fumitoshi Ochi¹, Takeharu Fujisawa¹, Takuya Ohmori¹, Takafumi Kawamura²

¹ Ship and Marine Technology Department, Products Development Center, IHI Corporation, Yokohama, Japan

²Department of System Innovation, Graduate School of Engineering, The University of Tokyo, Japan

ABSTRACT

A propeller hub vortex has strong low pressure core in its center. The low pressure of the core causes thrust deduction by pulling the propeller boss cap end. To predict the deduction is important when we design a ship.

We have applied numerical simulation method to predict it. Besides, we have measured the propeller thrust in case of non hub vortex condition and hub vortex condition. It is considered that the difference of these thrusts was caused by the hub vortex. The results of the computation and the experiment were compared, and a good agreement was confirmed.

The thrust deduction caused by the hub vortex was estimated to be about 5% by both computation and experiment. Further, it was shown that the thrust deduction can be decomposed into increase in the boss drag and decrease in the thrust of the blades. The simulation has predicted that the former is 2% and the latter is 2-3% of the total thrust.

Keywords

CFD, Propeller, Hub vortex

1 INTRODUCTION

Due to the recent rise in the energy cost, it is strongly required to develop ships which have higher energy efficiency than ever. There are many factors which have negative impacts on the ship performance. Propeller hub vortex is one of the factors. It has a strong low pressure core in the center, which causes thrust deduction by pulling the propeller boss cap end. The influence of hub vortex on the propeller performance must be considered in the design of a propeller design. However, it is difficult to predict analytically.

The purposes of this paper are to predict the influence of hub vortex flow by RANS simulation method and to verify the simulation results in comparison with experimental results.

2 NUMERICAL METHOD

The numerical method used in this study is almost same as used in the previous study (Kawamura et al.2004,

2008). The Navier-Stokes equation and the continuity equation are applied to analyze this situation as the governing equations. These equations are discretized by a finite volume method. We use commercial software FLUENT 6.3 as the solver. To analyze flow field in open water condition, only one blade was modeled and the periodic boundary conditions were used at the outer boundaries in circumferential direction. k-w SST model is used as turbulence model.

3 CONDITION OF COMPUTATION

We have used a propeller which has 5 blades and MAU blade section for this study. Principal particulars of the propeller are shown in Table 1.

Table 1 Principal particulars of MP423

Number of blades	5
Pitch Ratio	0.7
Expanded Area Ratio	0.65
Boss Ratio	0.18
Rake Angle (Degree)	0
Blade Section	MAU

We have used two types of computational domain as shown in Figure 1. The Propeller Open Test configuration type domain has the boss cap on the upstream side of the propeller. We call this configuration "POT". Prediction results by using this type domain was compared with propeller open test results. The Reversed Propeller Open Test configuration has the boss end on the downstream side. We call this configuration "R-POT". This type domain was used for prediction of the thrust deduction by hub vortex.

Computational space was defined as follows;

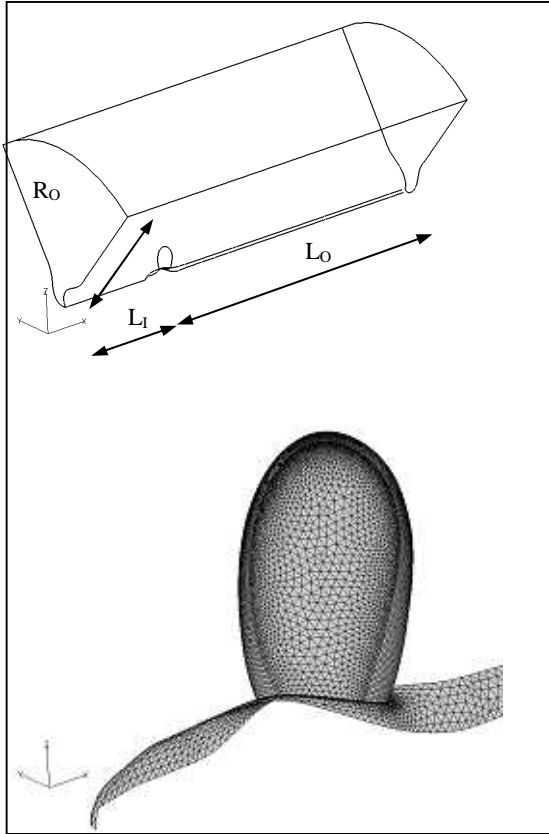
$$L_I = 2.2D$$

$$L_O = 5.2D$$

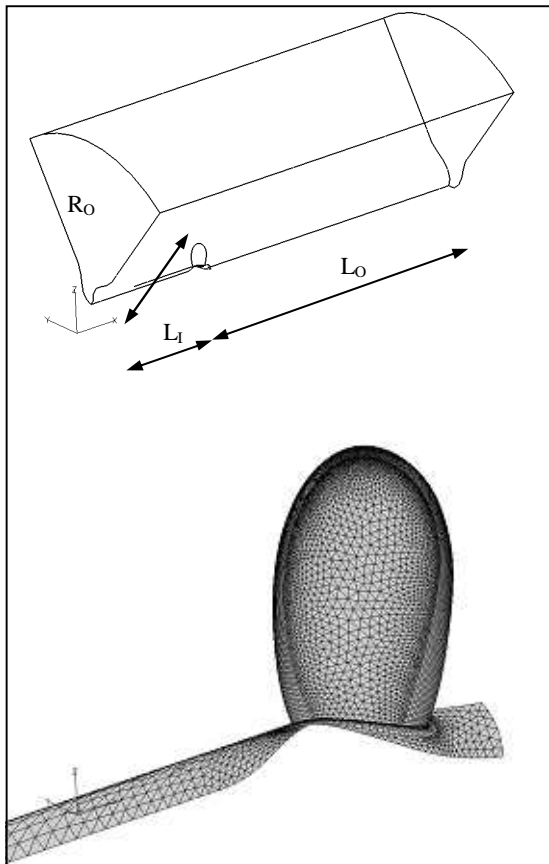
$$R_O = 3.0D$$

where L_I is the distance between propeller center and inflow boundary. Propeller center is defined at the intersection of the generator line and the axis of rotation. L_O is the distance between propeller center and outflow boundary, R_O is the distance between propeller center and

outer boundary. D is diameter of propeller.



POT configuration



R-POT configuration

Figure 1 Computational domain and mesh on the blade

4 EXPERIMENTAL MEASUREMENT

We have carried out experimental measurements to confirm accuracy of the simulation. We have used a model propeller of which diameter is 210mm. Reynolds number which is defined by the following formula was set to 3.0×10^5 in all experiments:

$$Rn(K) = \frac{C_{0.7R} \sqrt{V_A^2 + (0.7\pi nD)^2}}{\nu} \quad (1)$$

where $C_{0.7R}$ is chord length at 70% position of propeller radius, V_A is inflow velocity of propeller, n is revolution rate, D is propeller diameter, ν is kinematic viscosity.

At first, ordinary propeller open test was carried out. Test configuration is shown in Figure 2.

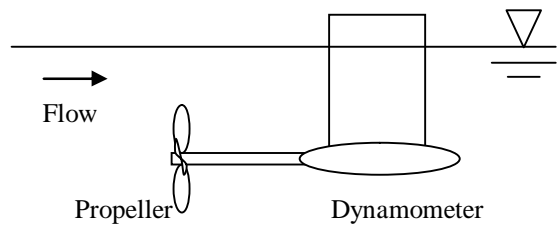


Figure 2 The test setting of Propeller Open Test

Secondly, reversed propeller open test was carried out for evaluation of the thrust deduction by hub vortex. In addition, reversed propeller open test with dummy shaft was carried out at third. Because it is necessary to correct the inflow velocity decreased by wake of propeller dynamometer in reversed propeller open test condition. Two types of test configurations are shown in Figure 3 and Figure 4. Actual model setting is shown in Figure 5.

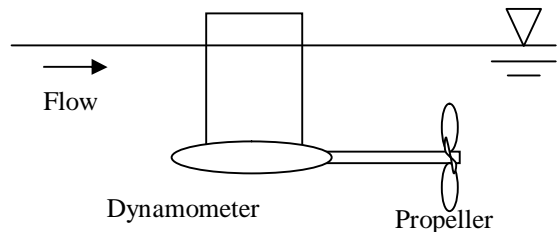


Figure 3 The setting of "Reversed Propeller Open Test"

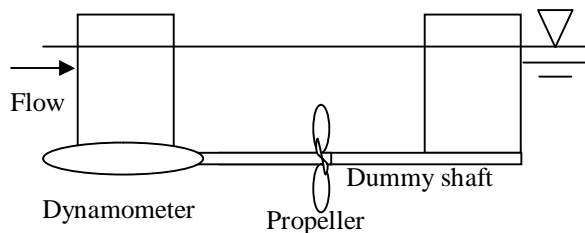


Figure 4 The setting of "Reversed Propeller Open Test" with dummy shaft

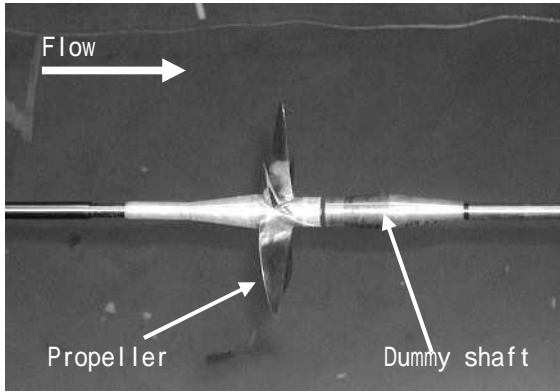


Figure 5 Actual setting of “Reversed Propeller Open Test” with dummy shaft

We also have carried out the experiment to measure the force acting on the propeller boss cap end. We have used CRP-POD type dynamometer shown in Figure 6. CRP-POD type dynamometer has two shafts which consist of inner shaft and outer shaft. Shaft forces are measured by each sensor. Actual test setting is shown in Figure 7. Boss cap force and propeller thrust were measured by each sensor. The experiments were carried out with propeller and without propeller, to evaluate the influence of hub vortex.

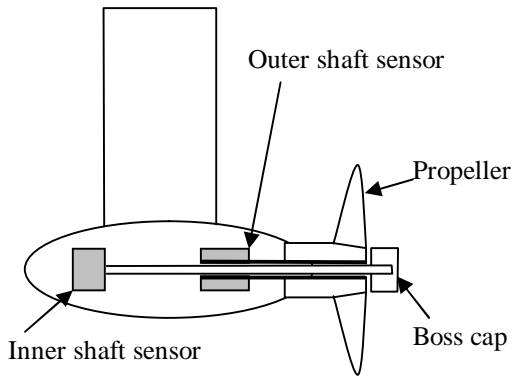


Figure 6 CRP-POD type dynamometer

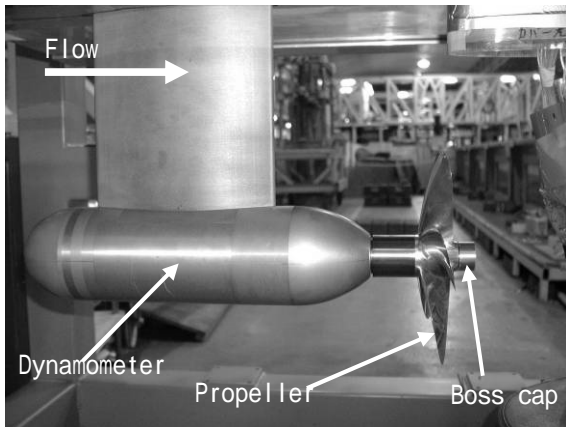


Figure 7 Actual setting of boss cap end force measurement

5 RESULTS

5.1 Comparison of CFD and EFD

We compared CFD and EFD result about POT condition to confirm accuracy. The comparison of propeller characteristics in POT condition is shown in Figure 8. Advance coefficient J , thrust coefficient K_T and torque coefficient K_Q is defined as follows;

$$J = \frac{V_A}{nD}, K_T = \frac{T}{\rho n^2 D^4}, K_Q = \frac{Q}{\rho n^2 D^5} \quad (2)$$

where T is propeller thrust, Q is propeller torque, ρ is density. Computational results do not involve the drag of shaft and boss cap. Experimental results involve the run idle correction. Computational results have good agreement with experimental results. Computational results are 1-3% different from experimental results.

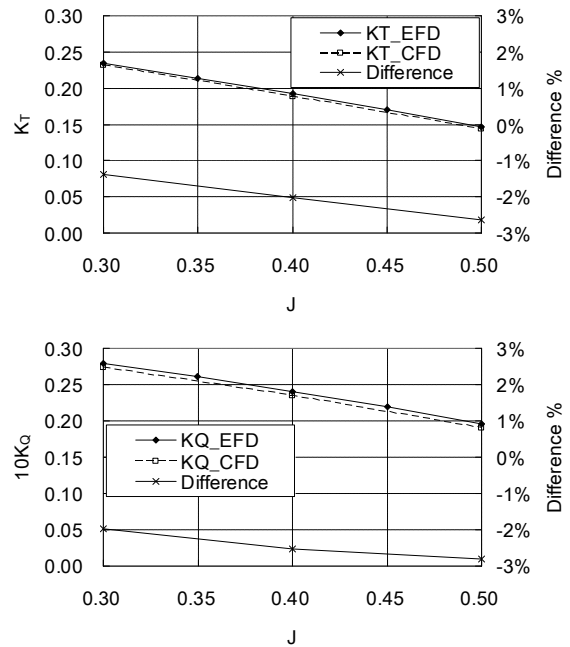


Figure 8 Comparison of “POT” propeller characteristics (above : K_T below : $10K_Q$)

Next, we considered the method for correcting the experimental results in R-POT condition, because experimental data include the influence of wake of the dynamometer. The comparison of K_T in R-POT condition and R-POT with dummy shaft condition is shown in Figure 9. From these data, the effective (corrected) advance coefficient J in the R-POT condition was estimated by using the identity of the thrust coefficient K_T . Correlation of the apparent and corrected advance coefficients is shown in Figure 10.

The comparison of propeller characteristics in R-POT condition is shown in Figure 11. Computational results involve the drag of shaft and boss end cap. Experimental results do not involve the run idle correction in order to compare under the same condition. The differences of K_T between computations and experiments are 2-4%, and the differences of K_Q are between -2% to 2%.

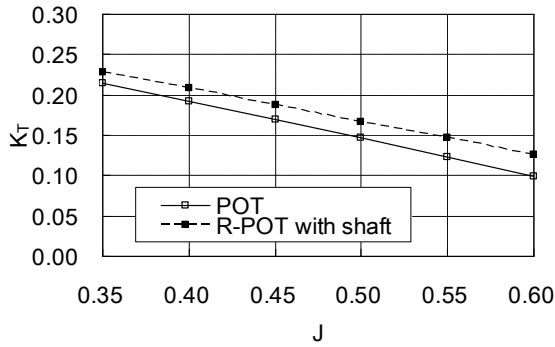


Figure 9 Comparison of K_T (experimental results)

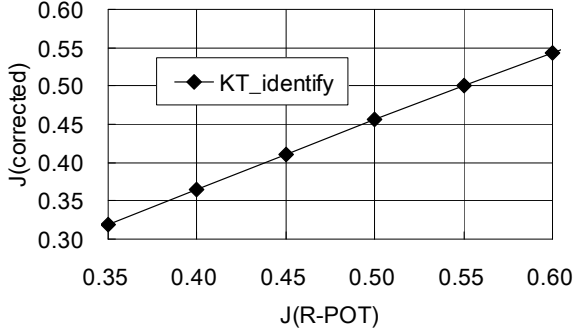


Figure 10 Correlation of J between "R-POT" and "POT" (experimental results)

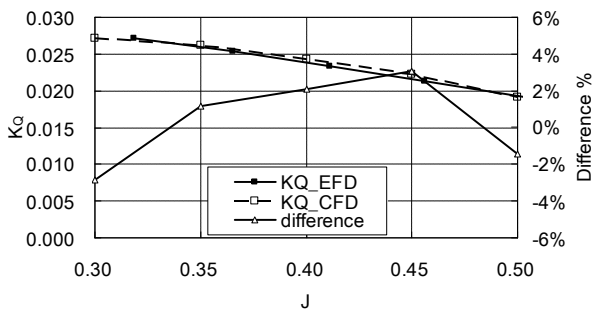
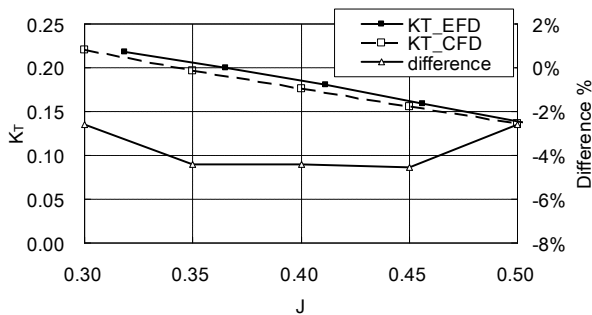


Figure 11 Comparison of "R-POT" propeller characteristics (above: K_T below: K_Q)

Next, we investigated the difference between "with shaft" and "without shaft" in R-POT condition to estimate the thrust deduction caused by hub vortex. Comparison of "R-POT condition" and "R-POT with shaft condition" is shown in Figure 12. In case of experiments, propeller thrust measured in "without shaft" condition was about 3-5% smaller than "with

shaft" condition. On the other hand, propeller thrust computed with boss end was about 5% smaller than that. It was considered that hub vortex caused these differences.

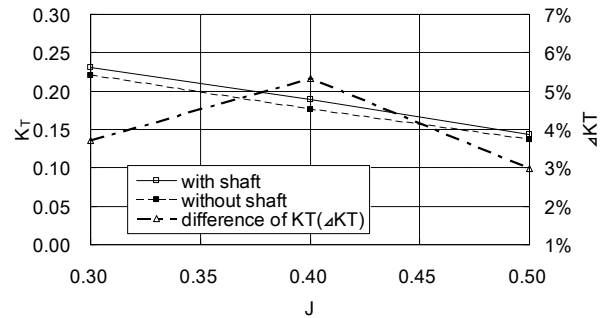
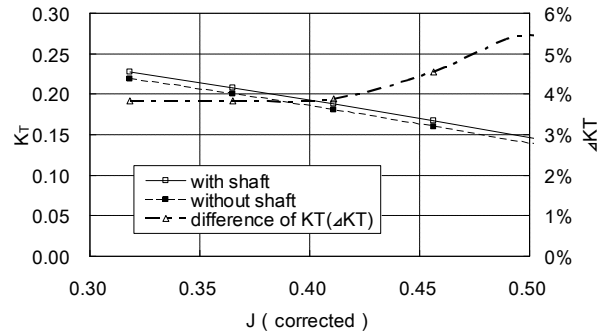


Figure 12 Comparison of propeller thrust coefficient with/without shaft (above: EFD below: CFD)

5.2 Components of propeller thrust deduction

The difference of thrust between POT condition and R-POT condition is caused by two factors, the suction drag caused by the hub vortex core $\Delta K_{T_{boss}}$ and the thrust deduction of propeller blades $\Delta K_{T_{blade}}$. Comparisons of these factors are shown in Figure 13. The suction drag was about 2% in all conditions. Next, we compared computed and measured boss cap drags. As shown in Figure 14, the computation shows good agreement with experimental data. Computed pressure distribution of POT condition and that of R-POT condition are compared in Figure 15 to find a reason of the thrust difference on blade. Negative pressure area computed in R-POT condition is wider than in POT condition. Negative pressure area in R-POT condition is extended from propeller trailing edge to boss end. Iso-surfaces of vorticity magnitude value of 20 are compared in Figure 16. It seems that vortex formations are different. In R-POT condition, vortex sheets extending from the trailing edges merge each other and form a hub vortex. On the other hand, such behavior is not present in POT condition. It is supposed that the vortex induces down wash on the blades, and that due to this down wash the propeller thrust on the blades in R-POT condition is smaller in R-POT condition than in POT condition.

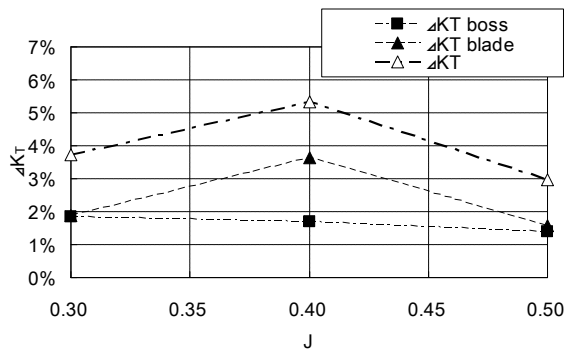


Figure 13 Contents of DK_T

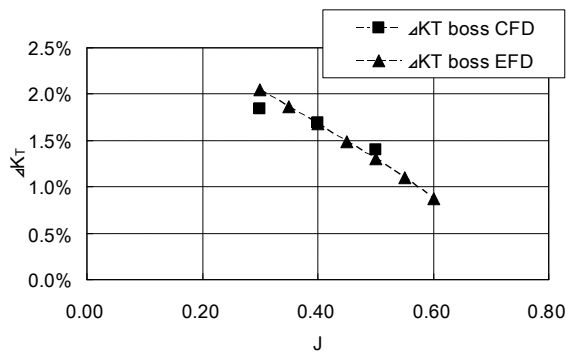


Figure 14 Comparison of boss cap drag

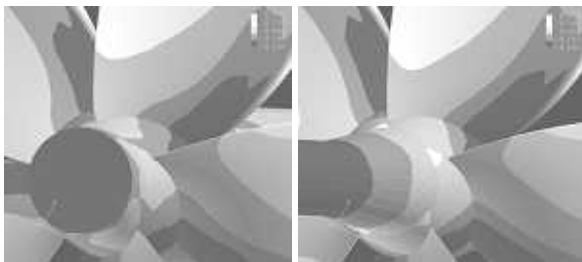


Figure 15 Pressure distribution on propeller blade at pressure side

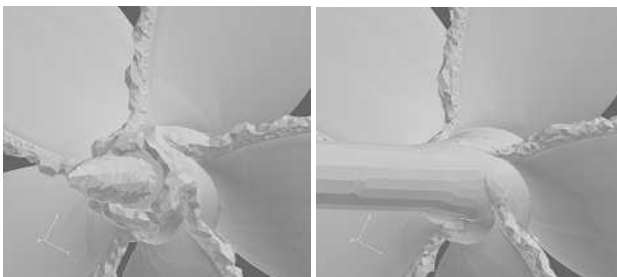


Figure 16 Isosurface of vorticity magnitude (magnitude=20)

6 CONCLUSION

In this paper, we have applied numerical simulation to the prediction of propeller hub vortex flow. The prediction of propeller thrust and torque were in good agreements with experimental results. The thrust

deduction was predicted to be 3-5% in this case. It was also shown that the thrust deduction can be decomposed into two components. One is the increased drag of the boss cap ΔKT_{boss} and the other is the decrease of the thrust of the blades ΔKT_{blades} . For the propeller tested in this study, ΔKT_{boss} was about 2% and ΔKT_{blades} was 2-3% of the total thrust.

REFERENCES

- T. Kawamura, T. Watanabe, Y. Takekoshi, M. Maeda, H. Yamaguchi (2004) 'Numerical Simulation of Cavitating Flow around a Propeller', Journal of the Society of Naval Architects of Japan Vol.195, pp.211-219. (in Japanese)
- T. Kawamura, T. Ohmori, (2008) 'Effect of the Reynolds Number on Propeller Performance in Open Water', Conference Proceedings the Japan Society of Naval Architects and Ocean Engineers May 2008 Volume 6, pp.189-192 (in Japanese)
- I. Funeno, T. Kawamura (2005). 'Application of CFD to Marine Propellers', The 5th Symposium on Marine Propellers. Tokyo, Japan. (in Japanese)